Sea State Characterization Using Experimental Synthetic Aperture Radar Raw Data in Two-Dimensions and the Modified Fractal Signature Method

Apostolos Kotopoulis, Basil Massinas, Georgios Pouraimis, Panayiotis Frangos*
School of Electrical and Computing Engineering, National Technical University of Athens,
9 Iroon Polytechniou Str., 157 73 Zografou, Athens, Greece
pfrangos@central.ntua.gr

***Abstract*—This paper presents a novel method for the characterization of the sea state using a set of raw experimental Synthetic Aperture Radar (SAR) data in two dimensions, i.e., in the "fast time" and "slow time" directions (as explained in the text) and the so-called "Modified Fractal Signature" (MFS) method. That is, experimental SAR radar signatures in the above two dimensions (i.e., "raw data" in the time domain) were provided to our research group by the Norwegian Institute of Defence (FFI Institute), Norway, which we processed and analyzed using the MFS method in a novel way, as presented in detail in this paper. The numerical results obtained here show an easy categorization of the sea surface as "calm sea" or "turbulent sea", thus establishing a very promising technique for the characterization of sea state in real time, as described in detail in the text.**

***Index Terms*—Synthetic aperture radar (SAR); Experimental backscattered SAR raw data; 3D processing and analysis of SAR raw data; Modified fractal signature (MFS) method; Fractal dimension; Sea state characterization.**

I. INTRODUCTION

The problem of characterization of the sea state by using backscattered electromagnetic (EM) waves or radar signals and fractal techniques is well known in the radar literature [1]–[14]. Here, the first question might arise, namely, why use fractal techniques for such a problem. The answer lies in the fact that for this problem of EM scattering from the sea surface, the latter can be considered either as a rough surface, which can be mathematically described by "random processes" (see, e.g., [15]) or as a "fractal surface" (see, e.g., [16]–[20]). More generally, fractal mathematics has been used in the literature to model rough surfaces for the problem of interaction of EM waves with them [21]–[24]. Furthermore, for interested readers, fundamental concepts about fractal mathematics can be found in [25]–[30].

In previous (recent) studies by our group in this area of research, we first dealt with simulation studies for the backscattering of EM radar waves from fractal surfaces [19], [20]. Furthermore, we examined the problem considered in this paper, i.e., the characterization of the sea surface from experimental SAR raw data, provided to us by FFI Institute, where we examined fractal properties of the backscattered one-dimensional (1D) SAR radar signatures (which are called in the SAR bibliography "range profiles"). In these papers of ours [13], [14], we examined the above-mentioned fractal properties of the "radar range profiles" by analyzing these range profiles "one by one", i.e., separately one from another (i.e., "1D analysis"). In [13], we examined the fractal properties of the "range profiles" in the time domain, while in [14] in the frequency domain. On the contrary, in the present paper by our research group, we examine the fractal properties of a "set of backscattered radar range profiles", that is "3D analysis" of these SAR raw data (as will be presented below, in this paper).

The structure of this paper is as follows. In Section II, we briefly present the real-field experimental SAR raw data provided to us by the FFI Institute. This is followed, in Section III, by the description of our proposed "three stages" of pre-processing of these data, necessary before the application of our "main sea state characterization algorithm", along with our numerical results, which show representative radar signatures at several stages of the above-mentioned "pre-processing" scheme. Furthermore, in Section IV, the "main sea state characterization algorithm", which is based on the "Modified Fractal Signature" (MFS) technique [31]–[34], applied to the pre-processed SAR raw data, described above, along with our numerical results "sea state characterization" is presented. Moreover, in Section V, a short discussion on the method proposed in this paper, which is considered to be fully novel, and also superior to our point of view, compared to the method proposed by our research group in [13], [14] is presented. Finally, in Section VI, future directions of this research are provided.

II. EXPERIMENTAL SAR RAW DATA

This paper uses SAR raw data recorded from sea clutter, which were collected during the "NEMO 2014" trials in Taranto, Italy, using PicoSAR X-band radar of the FFI (i.e.,

Manuscript received 18 August, 2022; accepted 19 November, 2022. This research was supported in part by National Technical University of Athens (NTUA)/EU under the "International Mobility Programme".

"Norwegian Institute of Defence", Oslo, Norway) as input to a specific SET Working Group. The experiment took place in Taranto bay in southern Italy on 23 and 24 September 2014. On the first day, the weather was quite windy (wind speed 10 m/s–12 m/s), thus creating a rather turbulent sea, compared to the second day, during which the sea surface was calm (wind speed 1 m/s–2 m/s).

The geometry of the sea state characterization problem is shown in Fig. 1. Here, a helicopter (with PicoSAR radar inside) moves vertically, with negligible horizontal velocity (helicopter movement from down to up, or vice versa), and the helicopter pilot kept the direction of the antenna beam up-wind (i.e., the direction of radar pulses - EM wave propagation in the opposite direction of the wind speed). The "PicoSAR" radar transmits Linear Frequency Modulation (LFM) radar pulses toward the sea, as shown in Fig. 1. Then it is able to record the backscattered "range profiles" from the sea surface as a function of the grazing angle θ_g (see Fig. 1). Here, M is the number of "range bins" in a range profile (where the "range profile" is the backscattered response in the time domain from the sea surface to one pulse of LFM emitted) and N is the total number of backscattered range profiles. Furthermore, here, the "range direction" is the direction of propagation of the EM waves and the "cross range" direction is the direction vertical to the previous one, while by "fast time" we mean the time interval between the "range bins" in a range profile and by "slow time" the time between subsequent range profiles.

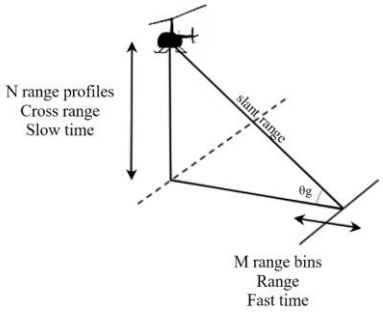

Fig. 1. Geometry of the sea state characterization problem, where the helicopter moves vertically transmitting PicoSAR radar electromagnetic (EM) pulses towards the sea.

On the first day (23/9/2014), the wind speed was reported in the range from 10 m/s to 12 m/s. That is, a high wind speed corresponding to a sea state 4 up to almost 5 (namely wave heights from 1.25 m up to 3 m). The helicopter moved vertically, where the grazing angles θ_g (see Fig. 1) were scanned in the range from 3 ° to 55 °, within a window of 20 ° in the horizontal (azimuthal) direction. The time of the full grazing angle span was approximately 4 minutes.

During the second day (24/9/2014), the wind speed was reported in the range from 1 m/s to 2 m/s, which sometimes died out locally. That is a very low wind speed that corresponds to a sea state 1 (wave heights from 0 m to 0.1 m). The helicopter moved vertically with the corresponding grazing angles in the range from 4 ° to 54 °, and, similarly with the first day, a slight drift in the azimuth pointing angle of the bore sight of no more than 20 °. The radar was set up to use a range to scene center (slant range) constant at 1850 m for all grazing angles.

III. Pre-Processing Data Scheme Proposed by Our Research Group

In this Section, the "three stages pre-processing scheme", introduced by our research group for the problem considered here (e.g., before the applying the "MFS sea state classification algorithm" to the radar data) is presented, along with the corresponding representative numerical results (produced by our research group).

Figure 2 presents two indicative range profiles for a grazing angle θ_g = 38.5 °, produced in the experiment described in Section II above. Namely, Fig. 2(a) presents an indicative range profile from "day 1/turbulent sea", and Fig. 2(b) a corresponding one from "day 2/calm sea". One can observe here that the maximum amplitude of the first (i.e., for "turbulent sea") is much higher than that of the "calm sea" (note that "relative amplitude information" between the two days of experiment, under consideration, will be kept, in some way, during the development of our "sea state classification algorithm" presented in this paper, and this is considered crucial for our proposed algorithm).

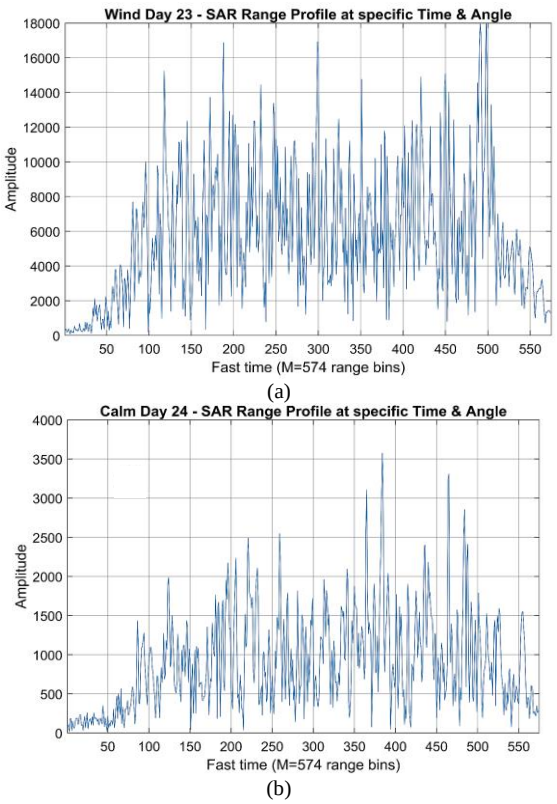

Fig. 2. Indicative range profiles from the experiment described in Section II: (a) "Day 1" (turbulent sea/"high amplitude values"), (b) "Day 2" (calm sea/"lower amplitude values").

Then, our "pre-processing scheme", proposed in this Section, consists of the following "three stages":

1. *Averaging* of range profiles (in this paper, by a factor N = 10) for noise reduction (i.e., to improve the "Signal-to-Noise Ratio" (SNR) of the signals). Please note that this technique is also sometimes referred to in "radar terminology" as "incoherent integration" of radar signals, i.e., integration of radar signals without "phase correction" [41]).

2. *Filtering* of signals to detect and remove "*outliers*" using the so-called "boxplot/IQR" statistical method [36]–[40]. Here, by the term "outliers" we mean some extreme (and erroneous) signal values, which are not justified by the statistical analysis of the majority of the signals values and which must be removed before further signal processing. Signal values that lie outside the outer fence are considered outliers

$$Upper\ fence = Q_3 + W * IQR, \tag{1}$$

where the values of Q_3 and IQR are calculated separately for each range profile. After extensive numerical experiments of ours in the available PicoSAR data, the optimal value of the parameter W ["Whisker parameter", usually in the range (1.5, 3)] [36]–[40] was found to be W = 2.25. This means that for this selected value of parameter W, most "outliers" were removed from the data without affecting the main body of the signal.

3. *Normalization* of signals by the maximum signal amplitude observed in the data (in this case also by the "*radar receiver dynamic range*"). Please note that in this way, *relative signal amplitude information is maintained, from "day 1" to "day 2"*, as also mentioned above. Min-max normalization linearly transforms all signal amplitudes into the range [0, 1]. For the data to be appropriate to be used as input to the "MFS sea state classification algorithm" of Section IV, they must be rescaled to the range [0, 255] using the formula

$$X' = (X - X_{min}) / (X_{max} - X_{min}) * 255, \tag{2}$$

where X_{max}-X_{min} is the "radar receiver dynamic range".

The indicative range profiles after the application of "stage 1" are shown in Fig. 3 (for "day 1/turbulent sea") and Fig. 4 (for "day 2/calm sea").

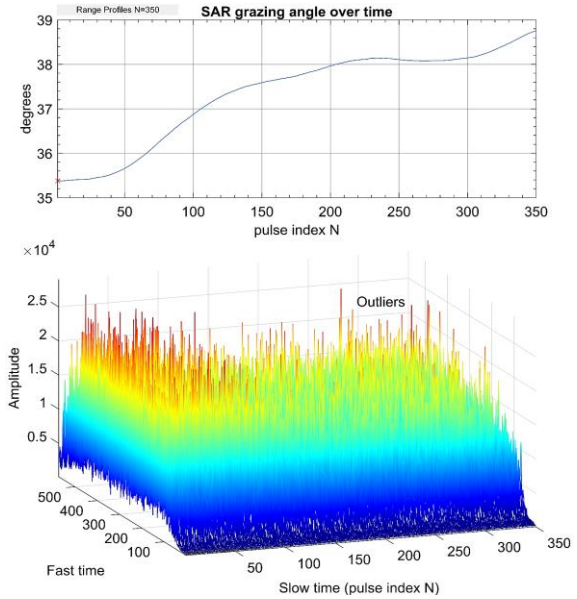

Fig. 3. Indicative range profiles in "3D representation" (e.g., a set of range profiles for 350 subsequent values of the "slow time" index N) after the application of "stage 1" ("averaging"). Here, for signals during "day 1/turbulent sea", "high signal values").

Note in Figs. 3 and 4 that in "day 1/turbulent sea" the amplitude of the signals is, in general, "much larger" than the corresponding values in "day 2/calm sea".

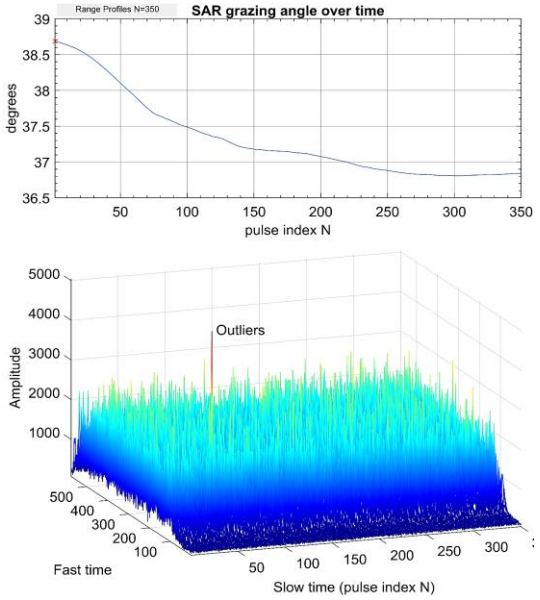

Fig. 4. Similarly to Fig. 3, but here for "day 2/calm sea", "low signal values".

Indicative range profiles after the application of "stage 2" ("*filtering of outliers*"), described above, are shown in Figs. 5 and 6 below ("outliers" successfully removed).

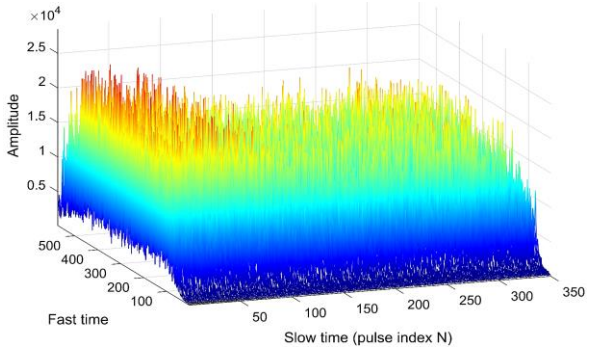

Fig. 5. Indicative range profiles in "3D representation" after the application of *"stage 2", ("filtering of the outliers")*. Here, for signals during "day 1/turbulent sea", "high signal values").

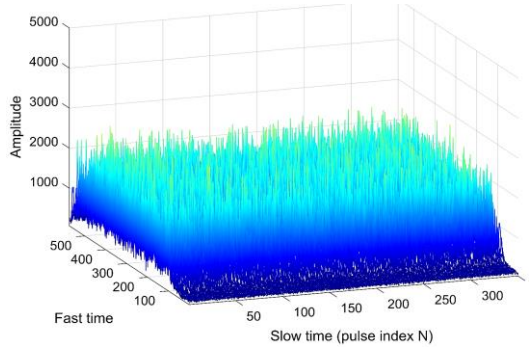

Fig. 6. Similarly to Fig. 5, but here for "day 2/calm sea").

Then, in the pre-processing data scheme described above, we are almost ready now to apply the "MFS classification algorithm". The word "almost" was added above, because the "3D data" derived in the way described above must now be normalized and rescaled to the range [0, 254], i.e., "stage 3", described above. Representative raw radar data in "3D-

form" and 2D-form after pre-processing stages are shown in Fig. 7 (case of turbulent sea) and Fig. 8 (case of calm sea).

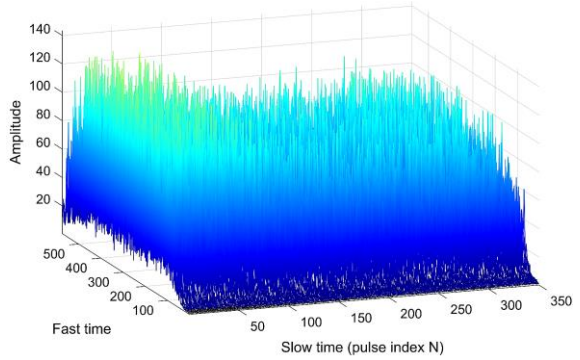

Fig. 7. Representative raw radar data in "3D form" after the pre-processing scheme described above are the final input to the MFS classification algorithm. Here, for "day 1/turbulent sea".

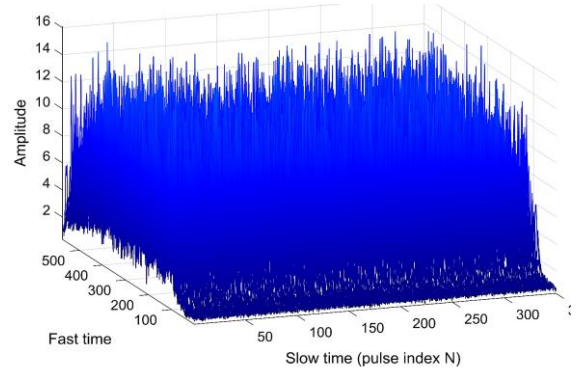

Fig. 8. Similarly, to Fig. 7, but here for "day 2/calm sea".

IV. Application of the "Modified Fractal Signature" (MFS) Method to Pre-Processed Radar Signals

The "Modified Fractal Signature" (MFS) method [31]–[34] is a well-known method used in the literature for image classification, such as texture and text analysis [31], [32], biomedical image classification [33], radar image classification [34], etc. The main idea behind it is to calculate the "fractal area" $A(\delta)$ of a rough surface using fractal techniques as a function of image resolution δ (in this method, δ also represents the "iteration order" in this iterative fractal technique). In this method, the "fractal area" is calculated by dividing the volume between the "upper surface" and the "lower surface" (of the 3D surface considered) by the height 2δ of that [32], hence its equivalent name of "blanket technique" (Fig. 9).

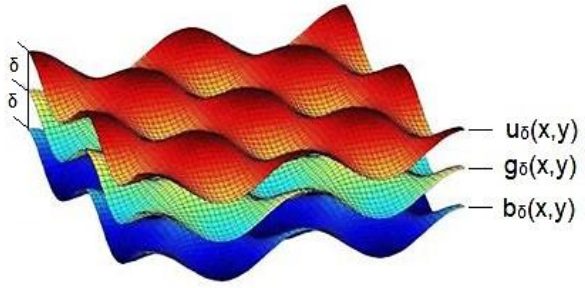

Fig. 9. Representation of the upper (u_δ) and lower (b_δ) blankets that cover the 3D radar signals (g_δ).

Once the "fractal area" of the rough 3D surface has been calculated as a function of iteration (image resolution) δ, the so-called "fractal dimension curve" $F_D(\delta)$ is calculated using well-known fractal techniques [31], [32] (note that the latter curve is also called in the bibliography as "modified fractal signature" (MFS) of the original rough surface). The mathematics of the MFS method can be found in [31], [32], and, in a very simple manner, for radar applications, in [34]. Note here that in [34] the "MFS classification method" is applied to "SAR radar images", and *not* to "SAR raw data", as in this paper, therefore it is a totally different method for "target classification".

When the "MFS classification method" is applied to the pre-processed 3D SAR raw data (according to the "pre-processing scheme" described in Section III), the "fractal signatures" curves $F_D(\delta)$ are shown in Fig. 10, where θg is the grazing angle, as shown in Fig. 1. The value D_μ shown in Fig. 10 is the average value obtained from all measurements of each fractal dimension curve $F_D(\delta)$.

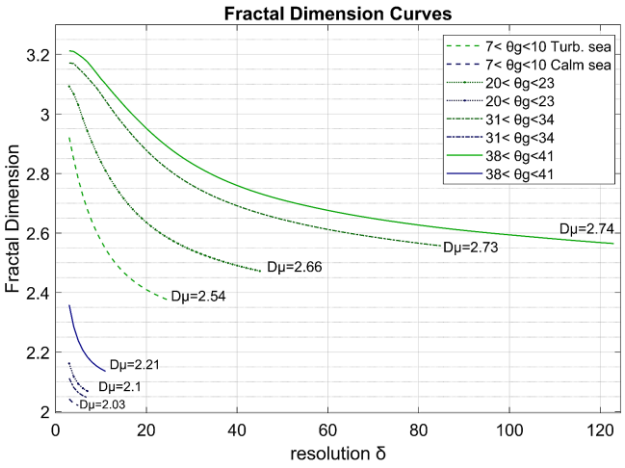

Fig. 10. Fractal signatures $F_D(\delta)$ obtained after the application of the "MFS classification method" to the "3D SAR raw radar" described in Section III (i.e., after the "pre-processing scheme").

Grazing angles with $\theta g > 41^\circ$ form fractal dimension curves that are exactly the same as the curve "$38^\circ < \theta g < 41^\circ$" and for that reason they are omitted from the plot. As we can see from Fig. 10, for the same sea state (e.g., turbulent sea), there is a dependency between fractal dimension curve and grazing angle. This dependency constantly decreases as the grazing angle increases. Above a certain value (e.g., $\theta g > 35^\circ$), the results of the fractal dimension are very slightly affected by the grazing angle.

Furthermore (and most important), from all these curves in Fig. 10, we can clearly see that, for all grazing angles considered here, the "turbulent sea" ("green curves" at the top of the figure/day 1) is very easily discriminated from the "calm sea" ("blue curves" at the bottom of the figure/day 2), which is very promising results for a later, fully automatic and "full scale", sea state characterization by the method described in this paper.

Furthermore, in Fig. 11, the "mean fractal dimension" D_μ is calculated in "real time" as a function of the grazing angle (θ_g) in the range from 20° to 50° degrees. In "real time", the proposed algorithm automatically reads the SAR raw data recorded for a duration of a 2.5 minutes of flight and every 3.5 seconds (namely every 3500 range profiles) it calculates one D_μ value from the fractal dimension curve $F_D(\delta)$ obtained after the application of the MFS method on

this set of 3500 range profiles.

Furthermore, the pink lines in Fig. 11 represent the 95 % prediction bounds based on our measurements. These prediction intervals indicate that we have a 95 % chance that any new observation will actually contain within the lower and upper prediction bounds. In other words, from Fig. 11 we can conclude that even without having the exact information on the grazing angle, if D_μ value is calculated between 2.0 and 2.3, then we have a probability of 95 % that the sea is in the sea state 1. While if D_μ value is calculated between 2.6 and 2.8, we have a probability of 95 % that the sea is in the sea state 4 up to 5.

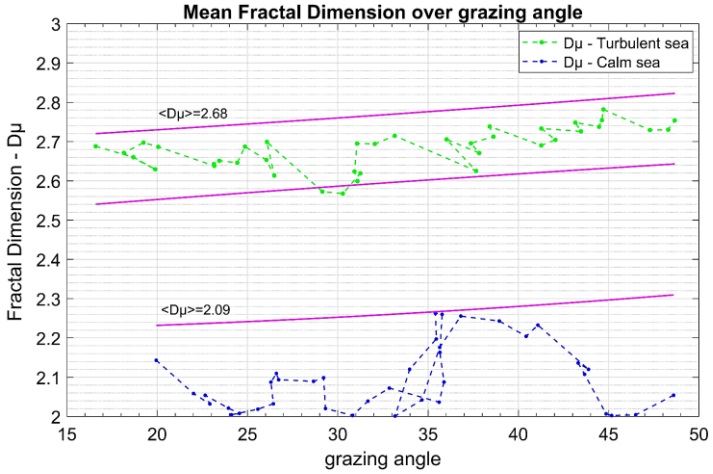

Fig. 11. Mean fractal dimension (D_μ) values are obtained every 3500 range profiles. The dashed "green line" represents the grazing angle route over the turbulent sea, while the dashed "blue line" represents the grazing angle route over the calm sea (grazing angle in degrees).

As a general trend, the amplitude of the backscattered electromagnetic (EM) wave increases with increasing grazing angle (θ_g) and this fact is also reflected here with the positive slope of the prediction bounds (pink lines), that is the increased grazing angles are associated with a probability of increased values of the "mean fractal dimension" (D_μ). If the grazing angle is known (e.g., the prediction bounds are calculated for a narrower grazing angle span), then the proposed method can provide a sea state characterization with even greater accuracy and certainty.

V. CONCLUSIONS

To summarize, in this paper, a novel method for automatic sea state characterization was presented by using airborne raw SAR radar data and fractal techniques (MFS algorithm). The raw data from the SAR experimental real field described above were pre-processed appropriately to improve the SNR of the signal and remove the unwanted "signal outliers", as described in detail in Section III. After these pre-processing steps, the "3D SAR raw data signals" (i.e., as a function of "fast time", in "range", and "slow time", in "cross range"), after "max-min normalization" and rescaling, were transformed into an appropriate range as input to the "Modified Fractal Signature" (MFS) classification method, thus obtaining very promising sea state classification results.

Note that in this method, the SAR raw data are normalized, for both days of sea observation, by the "radar dynamic range"; therefore, the information of the amplitude of the received radar signal is maintained between the two days of sea observation. In practical terms, i.e., for future possible practical exploitation of the method proposed in this paper, radar calibration is needed, as far as transmitted power, slant range, and grazing angle is concerned. These appear to be, in practical terms, some limitations to the method presented here, which, however, appears to be very promising for real-time and efficient sea state characterization by using airborne SAR radar techniques.

Finally, comparing the classification results of this paper with the corresponding results of ours based on our previous related research [13], [14], we have the following comments. Compared to the work in [13], here, the characterization of the sea state is provided by the "fractal dimension" criterion, which is a well-known measure of surface roughness widely used in the literature. Moreover, compared to the work in [14], the important advances of working with two-dimensional (2D) data (in this paper) rather than in one-dimensional (1D) data used in [14] were the following:

– Much more evident sea state characterization, i.e., much better separation of classification curves;

– Validity of our correct classification results for all grazing angle values, considered in this experiment by FFI (some drawbacks on those observed in the numerical results in [14]).

VI. FUTURE RESEARCH

Future related research can follow from this method for full sea state characterization, e.g., estimating the mean height of sea surface waves by using the above technique. Furthermore, the use of *simulated* SAR raw data, already available by our research group [19], [20], can be used for comparison (as opposed to the experimental SAR raw radar in real field used in this paper). Moreover, we could apply our method with real SAR radar data obtained from different airborne or spaceborne platforms. Finally, possible other fractal methods, except the MFS method used here, can be considered in future related studies, e.g., "Regny spectrum methods" [33], [35].

ACKNOWLEDGMENT

The authors would like to thank the SET-283 Working Group, and in particular, the FFI Institute (i.e., "Norwegian Institute of Defence", Oslo, Norway) for providing us with the real recorded sea clutter radar data, which were collected during the "NEMO 2014" trials in Taranto, Italy (see Figs. 1 and 2).

CONFLICTS OF INTEREST

The authors declare that they have no conflicts of interest.

REFERENCES

[1] T. Lo, H. Leung, J. Litva, and S. Haykin, "Fractal characterization of sea-scattered signals and detection of sea-surface targets", *IEE Proceedings F (Radar and Signal Processing)*, vol. 140, no. 4, pp. 243–250, 1993. DOI: 10.1049/ip-f-2.1993.0034.

[2] J. Hu, W.-W. Tung, and J. Gao, "Detection of low observable targets within sea clutter by structure function based multifractal analysis", *IEEE Transactions on Antennas and Propagation*, vol. 54, no. 1, pp. 136–143, 2006. DOI: 10.1109/TAP.2005.861541.

[3] J. Chen, T. K. Y. Lo, H. Leung, and J. Litva, "The use of fractals for modeling EM waves scattering from rough sea surface", *IEEE Transactions on Geoscience and Remote Sensing*, vol. 34, no. 4, pp. 966–972, 1996. DOI: 10.1109/36.508413.

[4] F. Berizzi, E. Dalle Mese, and G. Pinelli, "One-dimensional fractal model of the sea surface", *IEE Proceedings - Radar, Sonar and Navigation*, vol. 146, no. 1, pp. 55–64, 1999. DOI: 10.1049/ip-rsn:19990259.

[5] F. Berizzi and E. Dalle-Mese, "Fractal analysis of the signal scattered from the sea surface", *IEEE Transactions on Antennas and Propagation*, vol. 47, no. 2, pp. 324–338, 1999. DOI: 10.1109/8.761073.

[6] G. Lixin and W. Zhensen, "Fractal model and electromagnetic scattering from time-varying sea surface", *Electronics Letters*, vol. 36, no. 21, pp. 1810–1812, 2000. DOI: 10.1049/el:20001199.

[7] Z. Li and Y.-Q. Jin, "Bistatic scattering from a fractal dynamic rough sea surface with a ship presence at low grazing-angle incidence using the GFBM/SAA", *Microwave and Optical Technology Letters*, vol. 31, no. 2, pp. 146–151, 2001. DOI: 10.1002/mop.1383.

[8] F. Berizzi and E. Dalle-Mese, "Scattering from a 2-D sea fractal surface: Fractal analysis of the scattered signal", *IEEE Transactions on Antennas and Propagation*, vol. 50, no. 7, pp. 912–925, 2002. DOI: 10.1109/TAP.2002.800695.

[9] C. Yang and H. Zhou, "The study of electromagnetic scattering by a target with fractal rough surface", in *Proc. of 6th International Symposium on Antennas, Propagation and EM Theory*, 2003, pp. 488–491. DOI: 10.1109/ISAPE.2003.1276734.

[10] Y. Li, X. Lv, K. Liu, and S. Zhao, "Fractal-based target detection within sea clutter", *Acta Oceanol. Sin.*, vol. 33, no. 9, pp. 68–72, 2014. DOI: 10.1007/s13131-014-0519-1.

[11] A. Jayaprakash, G. Ramachandra Reddy, and N. S. S. R. K. Prasad, "Small target detection within sea clutter based on fractal analysis", *Procedia Technology*, vol. 24, pp. 988–995, 2016. DOI: 10.1016/j.protcy.2016.05.217.

[12] H. Pan, W. Zhang, W. Jiang, P. Wang, J. Yang, and X. Zhang, "Roughness change analysis of sea surface from visible images by fractals", *IEEE Access*, vol. 8, pp. 78519–78529, 2020. DOI: 10.1109/ACCESS.2020.2990161.

[13] A. Kotopoulis, B. Massinas, G. Pouraimis, and P. Frangos, "Sea state characterization using fractal techniques on experimental one-dimensional radar signatures", *Physical Sciences and Technology*, vol. 7, nos. 1–2, pp. 31–37, May 2020. DOI: 10.26577/phst.2020.v7.i1.05.

[14] G. Pouraimis, A. Kotopoulis, B. Massinas, and P. Frangos, "Sea state characterization using experimental one-dimensional radar signatures and fractal techniques", *Elektronika ir Elektrotechnika*, vol. 27, no. 3, pp. 71–77, Jun. 2021. DOI: 10.5755/j02.eie.28906.

[15] P. Beckmann and A. Spizzichino, *The Scattering of Electromagnetic Waves from Rough Surfaces*. Norwood, MA, Artech House, Inc., 1987.

[16] D. L. Jaggard and X. Sun, "Scattering from fractally corrugated surfaces", *Journal of the Optical Society of America A*, vol. 7, no. 6, pp. 1131–1139, 1990. DOI: 10.1364/JOSAA.7.001131.

[17] S. Savaidis, P. Frangos, D. L. Jaggard, and K. Hizanidis, "Scattering from fractally corrugated surfaces using the extended boundary condition method", *Journal of the Optical Society of America A*, vol. 14, no. 2, pp. 475–485, 1997. DOI: 10.1364/JOSAA.14.000475.

[18] D. L. Jaggard, A. D. Jaggard, and P. V. Frangos, "Fractal electrodynamics: Surfaces and superlattices", in *Frontiers in Electromagnetics*. Wiley-IEEE Press, 2000, pp. 1–47. DOI: 10.1109/9780470544686.ch1.

[19] A. D. Kotopoulis, A. Malamou, G. Pouraimis, E. Kallitsis, and P. V. Frangos, "Characterization of rough fractal surfaces from backscattered radar data", *Elektronika ir Elektrotechnika*, vol. 22, no. 6, pp. 61–66, 2016. DOI: 10.5755/j01.eie.22.6.17226.

[20] G. Pouraimis, A. Kotopoulis, E. Kallitsis, and P. Frangos, "Characterization of three-dimensional rough fractal surfaces from backscattered radar data", *Elektronika ir Elektrotechnika*, vol. 23, no. 4, pp. 45–50, 2017. DOI: 10.5755/j01.eie.23.4.18721.

[21] A. K. Sultan-Salem and G. L. Tyler, "Validity of the Kirchhoff approximation for electromagnetic wave scattering from fractal surfaces", *IEEE Transactions on Geoscience and Remote Sensing*, vol. 42, no. 9, pp. 1860–1870, 2004. DOI: 10.1109/TGRS.2004.832655.

[22] R. Xin-Cheng and G. Li-Xin, "Fractal characteristics investigation on electromagnetic scattering from 2-D Weierstrass fractal dielectric rough surface", *Chinese Physics B*, vol. 17, no. 8, p. 2956, 2008. DOI: 10.1088/1674-1056/17/8/032.

[23] A. Iodice, A. Natale, and D. Riccio, "Kirchhoff scattering from fractal and classical rough surfaces: Physical interpretation", *IEEE Transactions on Antennas and Propagation*, vol. 61, no. 4, pp. 2156–2163, 2013. DOI: 10.1109/TAP.2012.2236531.

[24] N. Lin, H. P. Lee, S. P. Lim, and K. S. Lee, "Wave scattering from fractal surfaces", *Journal of Modern Optics*, vol. 42, no. 1, pp. 225–241, 1995. DOI: 10.1080/09500349514550181.

[25] K. Falconer, Fractal Geometry: Mathematical Foundations and Applications. Wiley, 1990. DOI: 10.2307/2532125.

[26] B. B. Mandelbrot, *The Fractal Geometry of Nature*. New York: W. H. Freeman and Company, 1977.

[27] B. B. Mandelbrot, *Fractals: Form, Chance and Dimension*. W. H. Freeman and Company, 1977.

[28] B. Mandelbrot, "How long is the coast of Britain? Statistical self-similarity and fractional dimension", *Science*, vol. 156, no. 3775, pp. 636–638, 1967. DOI: 10.1126/science.156.3775.636.

[29] R. Esteller, G. Vachtsevanos, J. Echauz, and B. Lilt, "Comparison of fractal dimension algorithms using synthetic and experimental data", in *Proc. of ISCAS'99, IEEE International Symposium on Circuits and Systems*, 1999. DOI: 10.1109/ISCAS.1999.778819.

[30] B. Li, Y. Xu, J. Zhang, and L. Cui, "Study on calculation models of curve fractal dimension", in *Proc. of 6th International Conference on Natural Computation (ICNC 2010)*, 2010, pp. 3072–3079. DOI: 10.1109/ICNC.2010.5584690.

[31] S. Peleg, J. Naor, R. Hartley, and D. Avnir, "Multiple resolution texture analysis and classification", *IEEE Transactions on Pattern Analysis and Machine Intelligence*, vol. PAMI-6, no. 4, pp. 518–523, Jul. 1984. DOI: 10.1109/TPAMI.1984.4767557.

[32] Y. Y. Tang, H. Ma, D. Xi, X. Mao, and C. Y. Suen, "Modified fractal signature (MFS): A new approach to document analysis for automatic knowledge acquisition", *IEEE Transactions on Knowledge and Data Engineering*, vol. 9, no. 5, pp. 747–762, 1997. DOI: 10.1109/69.634753.

[33] N. B. Ampilova, E. Y. Gurevich, and I. P. Soloviev, "Application of modified fractal signature and Regny spectrum methods to the analysis of biomedical preparation images", in *Proc. of CEMA'11 International Conference*, 2011, pp. 96–100.

[34] A. Malamou, C. Pandis, P. Frangos, P. Stefaneas, A. Karakasiliotis, and D. Kodokostas, "Application of the modified fractal signature method for terrain classification from synthetic aperture radar images", *Elektronika ir Elektrotechnika*, vol. 20, no. 6, pp. 118–121, 2014. DOI: 10.5755/j01.eee.20.6.7281.

[35] A.-M. Lazar and R. Ursulean, "Further applications of the fractal spectra of the EEG signals", *Elektronika ir Elektrotechnika*, vol. 82, no. 2, pp. 45–48, 2008.

[36] J. Han, M. Kamber, J. and Pei, *Data Mining: Concepts and Techniques*, 3rd ed. Morgan Kaufmann Publishers, Burlington, 2011.

[37] J. W. Tukey, *Exploratory Data Analysis*. Addison-Wesley Publishing Company, 1977.

[38] A. Papoulis, *Probability, Random Variables, Stochastic Processes*, 3rd ed. New York, NY, USA: McGraw-Hill, 1991.

[39] F. Argenti, A. Lapini, T. Bianchi, and L. Alparone, "A tutorial on speckle reduction in synthetic aperture radar images", *IEEE*

Geoscience and Remote Sensing Magazine, vol. 1, no. 3, pp. 6–35, 2013. DOI: 10.1109/MGRS.2013.2277512.

[40] C. Wang, J. Caja, and E. Gómez, "Comparison of methods for outlier identification in surface characterization", *Measurement*, vol. 117, pp. 312–325, 2018. DOI: 10.1016/j.measurement.2017.12.015.

[41] M. I. Skolnik, *Introduction to Radar Systems*, 2nd ed. McGraw-Hill Book Company, New York, 1980.